Laser-enhanced negative ion mass spectroscopy for weakly electron-attaching species

Lal A. Pinnaduwage*,[1], Kannadaguli Nagesha, Yifei Zhu, Michelle V. Buchanan, Gregory B. Hurst

Oak Ridge National Laboratory, Oak Ridge, TN 37831-6122, USA

Abstract

We report the first observation of efficient negative ion formation in excimer-laser irradiated benzene and toluene. These negative ions were formed via enhanced electron attachment to highly-excited states produced by the laser radiation. The potential of this technique as an analytical tool is discussed. Due to the general nature of the enhanced electron attachment mechanism involved, this technique can be expected to be applicable for a wide variety of molecules. (Int J Mass Spectrom 193 (1999) 77–86) © 1999 Elsevier Science B.V.

Keywords: Negative ions; Rydberg states; Electron attachment; Mass spectrometry; Laser

1. Introduction

Analytical techniques that employ electron capture processes are widely used for high sensitivity detection of compounds [1,2]. These techniques, including electron capture chromatographic detectors and electron capture chemical ionization mass spectrometry, generally detect compounds with a propensity to capture low energy electrons. These compounds include those with electrophilic substituents, such as polychlorinated biphenyls, and those with low-lying unoccupied molecular orbitals, such as condensed ring aromatic hydrocarbons [3]. However, for compounds with smaller electron capture cross sections,

including polychlorinated biphenyls with few chlorine atoms and nonchlorinated volatile organics, those analytical methods are considerably less sensitive. For example, the electron attachment rate constant for highly chlorinated molecules can be as large as 10^{-7} cm^3 s^{-1}, whereas for many other molecules it can be 10^{-12} cm^3 s^{-1} or less [4]. Therefore, although conventional negative-ion based analytical techniques (which depend on negative ion formation via electron attachment to analyte molecules in their ground electronic states) can have extremely high sensitivities for the detection of certain species, they are not suitable for the detection of many other species.

During the past several years we conducted electron attachment studies on molecules excited to highly excited electronic states via laser excitation (see [5–7], and references cited therein) and discharge-based excitation [8,9]. These studies have shown that

---

* Corresponding author. E-mail: llp@ornl.gov
[1] Also at Department of Physics, University of Tennessee, Knoxville, TN 37996.

electron attachment rate constants in the range from $>10^{-7}$ [6] to 10^{-3} cm^3 s^{-1} [10] are associated with high-Rydberg states of a number of molecules for which the rate constants for the corresponding ground electronic states are $<10^{-12}$ cm^3 s^{-1}. Such an enhancement of many orders of magnitude in electron attachment holds promise to be of significant use for analytical purposes, and we have initiated studies to explore this possibility. In this article we report the preliminary results on negative ion formation via enhanced electron attachment to laser-excited benzene and toluene.

Prior studies have examined negative ion formation via electron attachment to ground states of benzene and toluene. Only a weak signal due to the $C_6H_5^-$ ion that peaked around 8 eV electron energy was observed in basic electron attachment studies on benzene in the ground electronic state [11,12], where a cross section of $\approx 10^{-19}$ cm^2 was reported. Nitrogen-enhanced negative ion formation in benzene in an electron impact experiment [13] yielded mainly the $C_2H_2^-$ and other analytically insignificant low-mass ions with $m/z < 30$. In an electron impact mass spectrometric study using 20–70 eV electrons [14], mainly the low-mass fragment anions together with weaker signals for high-mass fragment anions were observed in benzene and toluene.

In our electron attachment studies on laser excited molecules, the molecules were excited to energies above their ionization thresholds (within a few electron volts), by two- or three-photon excitation. Our earlier experiments (see [5,6], and references cited therein) were conducted under fairly high pressure (tens or hundreds of torr), where a small amount of the order of 10^{-2} Torr of the target gas was mixed in a buffer gas such as N_2 or Ar. The buffer gas was not affected by the laser radiation, and the high pressure environment allowed the electrons produced via photoionization of the target gas to drift through the laser-irradiated region; these electrons attached to the excited molecules produced by the same laser pulse. The identity of the excited states produced via excitations to energies above the ionization threshold of the target gas was not clear until recently, since it had been assumed that superexcited states [15] of mole-
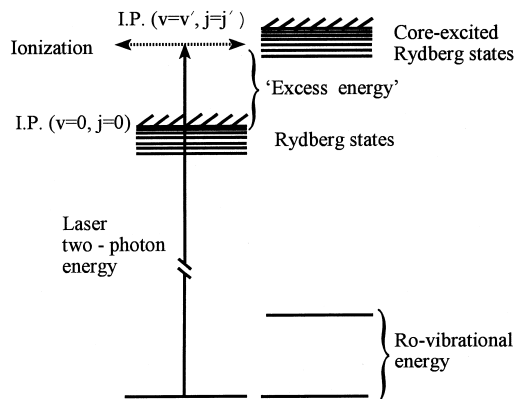

Fig. 1. Laser photon interactions with the continuum/discrete molecular states which lead to the formation of core-excited Rydberg states; v and j denote vibrational and rotational states.

cules lying above the ionization threshold would decay within subnanoseconds.

However, we recently showed that excitations to energies above and within a few electron volts of the ionization threshold leads to the formation of core-excited high-Rydberg states with lifetimes in the microsecond range [16]. By comparing the intensities of the ionization and the high-Rydberg signals of Fig. 2(a) and (b) in [16], we estimate that 10%–20% of the excitations of benzene to energies above the ionization thresholds by the KrF laser line end up in long-lived neutral states. Since the total energy of these states exceed the lowest ionization potential of the molecule, they can be called superexcited HR states or core-excited HR states. During the past few years, evidence for long-lived neutral states with total energies exceeding the lowest ionization threshold has accumulated also from the area of zero kinetic energy (ZEKE) photoelectron spectroscopy [17–19]. In general, when a molecule is excited to an energy above its lowest ionization threshold (within a few electron volts of the threshold), a significant fraction of the excitations can lead to long-lived neutral states where the excited electron is in a bound high-Rydberg (HR) state with the ion core carrying the "excess energy," see Fig. 1; also see, e.g. [20].

Therefore, the following processes can occur when benzene is excited to an energy above its ionization threshold via two-photon absorption:

$$C_6H_6^+ + e^- \qquad\qquad (1a)$$

$$C_6H_6 + 2h\nu \rightarrow$$
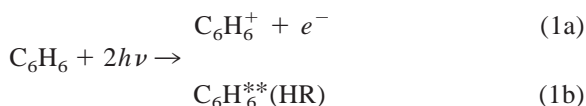
$$C_6H_6^{**}(HR) \qquad\qquad (1b)$$

where, $C_6H_6^{**}$(HR) denotes a superexcited high-Rydberg molecule. In our earlier high pressure experiments [5,6], such a high-Rydberg molecule captured an electron produced by photoionization by the same laser pulse [5]. However, in those high pressure experiments mass spectrometric identification of the negative ions was not possible.

We recently constructed an apparatus where the negative ions produced under lower pressure conditions (of the order of 10^{-2} Torr) via laser excitation were extracted to a time-of-flight mass spectrometer for mass identification; these experiments were conducted either using a gas cell [21] or a pulsed molecular beam [7]. In these experiments the negative ions were also produced via the capture of a weakly bound electron from one Rydberg molecule by an adjacent Rydberg molecule [7]. Our most recent experiments suggest that some photoionization electrons may be trapped by space charge fields, and may also contribute to electron attachment in these experiments.

In the present article we present negative ion mass spectra obtained in the above mentioned apparatus using both the gas cell and the pulsed valve. An inherent advantage of this laser excitation mechanism is that only one laser is needed to produce the excited states, since wavelength tunability is not required. It must also be noted that the present experiments do not utilize the full potential of electron attachment to highly excited states, since most of the attaching electrons are provided by excited molecules themselves. Therefore, large number densities of Rydberg states are needed to produce negative ions in the present experiments. The extremely large cross sections associated with the high-Rydberg states could be fully utilized by providing external electrons for attachment. Such experiments are being planned.

In this article we show that negative ions of benzene and toluene can be efficiently produced by the laser-enhanced process. Since the method relies on excitation of the molecules to energies above the ionization threshold, we can observe positive ions produced via photoionization as well.

2. Experimental

Negative ion spectra from laser-irradiated benzene and toluene were obtained with two different experimental arrangements. In one arrangement, the negative ions were produced in a static gas cell. This original arrangement was described in a previous publication [21]; in the present study, an additional ion lens system was installed at the gas cell exit in order to optimize the transmission of the ions, see Fig. 2(a). Briefly, the laser beam propagated between the ion exit pin hole in the gas cell and an electrode, and exited through an optical window. Ions produced by the laser beam were pushed out of the gas cell by an "extraction pulse" applied to the electrode (after a time delay of $\approx 0.5 \ \mu$s from the laser pulse), and arrived in between the two grids at the entrance to the time-of-flight (TOF) mass spectrometer. A second voltage pulse ("start pulse") applied to grid #1 after a time delay of 10–50 μs from the first pulse injected the ions to the TOF; grid #2 placed close to the TOF entrance was grounded, and hence electrically shielded the TOF field from the ion injection field. The timings of the laser, the extraction pulse, and the start pulse were controlled by a Stanford Research (Sunnyvale, CA) model DG 535 pulse/delay generator. Comstock (Oak Ridge, TN) power supplies of model numbers RS-112 and RS-110 were used to provide the extraction and start pulses. By reversing the polarities of the pulsed power supplies, positive ions produced via laser photoionization could be detected as well. Gas pressure in the cell was in a range from $\approx 10^{-2}$ Torr to 5×10^{-2} Torr.

The other experimental arrangement used in the present studies employed a pulsed beam valve and is shown schematically in Fig. 2(b); this apparatus was used earlier to obtain information on the lifetimes of the superexcited HR states produced by laser irradiation [16,22]. A Jordan (Grass Valley, CA) model C-211SS pulsed molecular valve was employed and the pulsed molecular beam was intercepted between
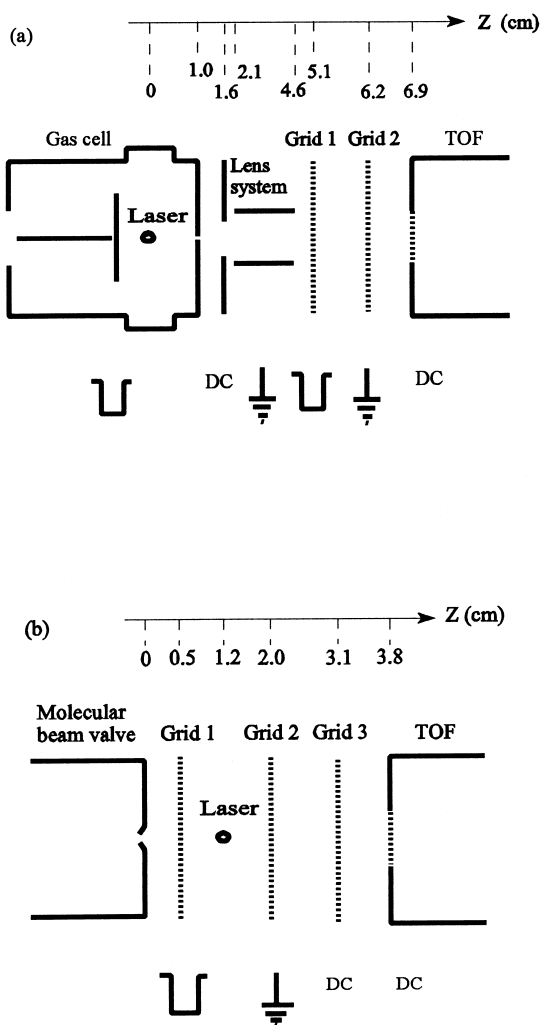
Fig. 2. Two experimental arrangements used. (a) The gas cell configuration: The negative ions produced by the interaction of laser-excited species were pushed out through a pinhole using a delayed extraction pulse; these ions were focused to the region between the grids #1 and #2 using a lens system and then were injected to the TOF by a start pulse applied to grid #1. (b) The pulsed beam valve configuration: Ion produced by the laser were injected to the TOF using a delayed start pulse applied to grid #1. The voltage on grid #3 was adjusted to yield the optimum ion transmission. The grid #3 was needed for the studies [16,22] of the dynamics of the excited states responsible for the negative ion formation process, but is not mandatory for the present studies.

the grids #1 and #2 by the pulsed laser beam. Negative (or positive) ions produced by the laser beam were pushed in to the TOF by applying a negative (or positive) pulsed voltage to the grid #1;

this we will refer to as the start pulse. The rising edge of the start pulse was taken to be $t = 0$ for the flight time of the ions. The start pulse generated by Comstock model RS-110 pulsed power supply was ≈ 100 V in height and ≈ 3.5 μs of duration. In the present experiments, grid #2 was grounded and grid #3 was kept at a voltage of $100-500$ V to optimize the ion transmission. The timings of the pulsed molecular valve, the laser, and the extraction pulse were controlled by a Stanford Research model DG 535 pulse/delay generator.

The pulsed molecular beam valve was operated with low backing pressure ($2-50$ Torr) and without any carrier gas. The gas pulse was ≈ 200 μs long and for a backing pressure of 10 Torr we estimate the gas pressure in the interaction region to be $\approx 10^{-3}$ Torr. The background pressure was $\approx 5 \times 10^{-8}$ Torr. We estimate the molecular beam velocity to have a broad distribution with average velocities around $400-500$ m s^{-1}.

A Lumonics model EX-500 excimer laser was used for the gas cell experiments, and a Lambda Physik model EMG 102 excimer laser was used for the pulsed beam valve experiments; the pulse durations were ≈ 20 ns [full width at half maximum (FWHM)]. A uniform cross section of the laser beam was reduced in cross section using a telescope arrangement with two fused silica lenses of focal lengths of 30 and 10 cm. The resulting laser beam cross section was ≈ 0.02 cm^2. It propagated between grids #1 and #2 [see Fig. 2(b)] and exited through an optical window. As in the gas cell apparatus, the laser beam did not hit any metal surfaces in the interaction region so that electrons were not produced by photoelectric emission. The laser was operated at a repetition rate of 2 Hz and each ion spectrum was obtained by averaging 32 laser shots. However, in most cases the signals were strong enough so that even a single shot was sufficient to obtain a TOF spectrum. The flight tube voltage was kept at 900 V. The ions were detected by a using a R.M. Jordan model #748-25 microchannel plate detector.

Benzene and toluene purchased from Aldrich Chemical Company (Milwaukee, WI) with stated purities of 99.99% and 99.97% respectively; samples
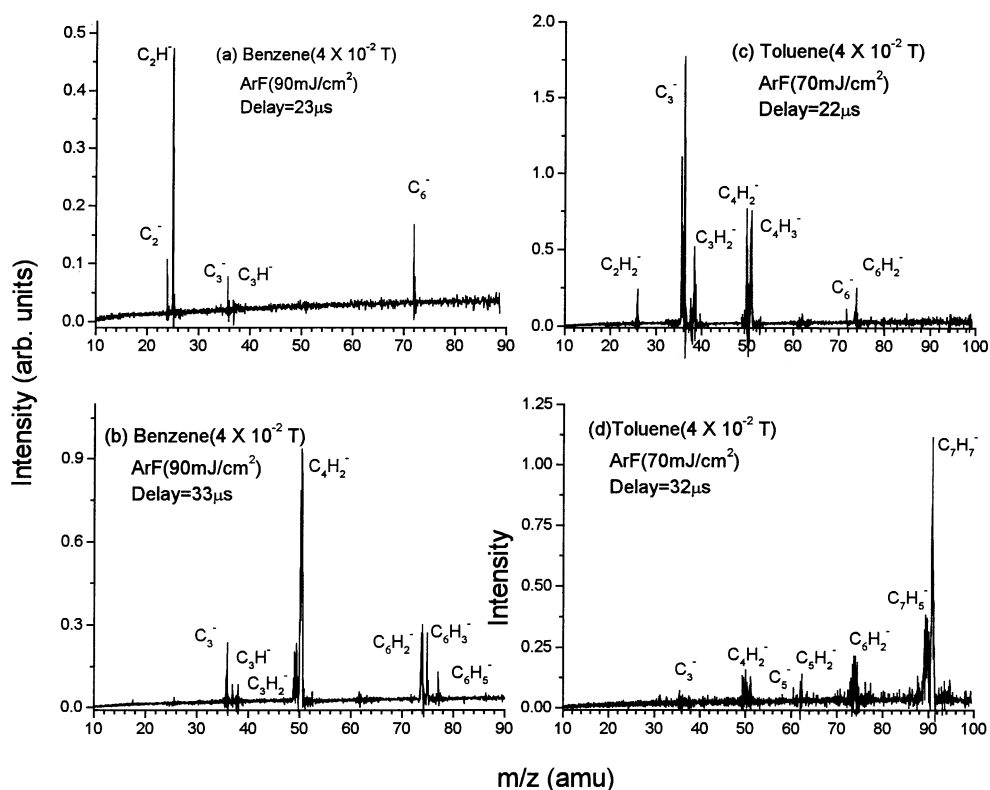
Fig. 3. ArF laser-induced negative ion mass spectra for benzene and toluene obtained with the gas cell arrangement. The time delay indicated in each figure is the time between the laser pulse and the start pulse applied to grid #1 [see Fig. 2(a)]; this is basically the time taken for the ions to arrive at the region between grids #1 and #2. Therefore, predominantly light ions were observed at shorter time delays and predominantly heavier ions were observed at longer time delays.

were degassed by subjecting them to a number of freeze–pump–thaw cycles prior to usage.

3. Results and discussion

Negative ion spectra obtained with the gas cell [see Fig. 2(a)] are shown in Fig. 3; it shows data for benzene and toluene at the ArF laser line. In these experiments, the static gas pressure in the gas cell was ≈ 0.04 Torr. We see that the negative ion spectra have a series of negative ion clusters separated by roughly the mass of a C atom; the C^- ion was not observed, and the C_5^- ion was also weak. The spectra for toluene were quite similar to those of benzene except, of course, for the presence of C_7^- ion for toluene.

The relative intensities of the ions measured with

the gas cell are skewed since not all the ions are detected with same efficiency. It must be noted that the time delays indicated in Fig. 3 represent the delay of the application of the start pulse with respect to the laser pulse (start pulse is applied to grid #1 to push the ions into the TOF, and the rising edge of this pulse is taken to be $t = 0$ for the flight time of the ions in the TOF). This basically represents the time taken by the ions to reach the region between the grids #1 and #2: At shorter delays mostly the lighter ions had arrived in the extraction region and thus the mass spectrum predominantly contains lighter ions. At longer delays, heavier ions dominate the mass spectrum. Also to be noted is that the "extraction pulse" on the electrode inside the gas cell (to push the ions out of the gas cell) was turned on ≈ 0.5 μs after the laser pulse. In order
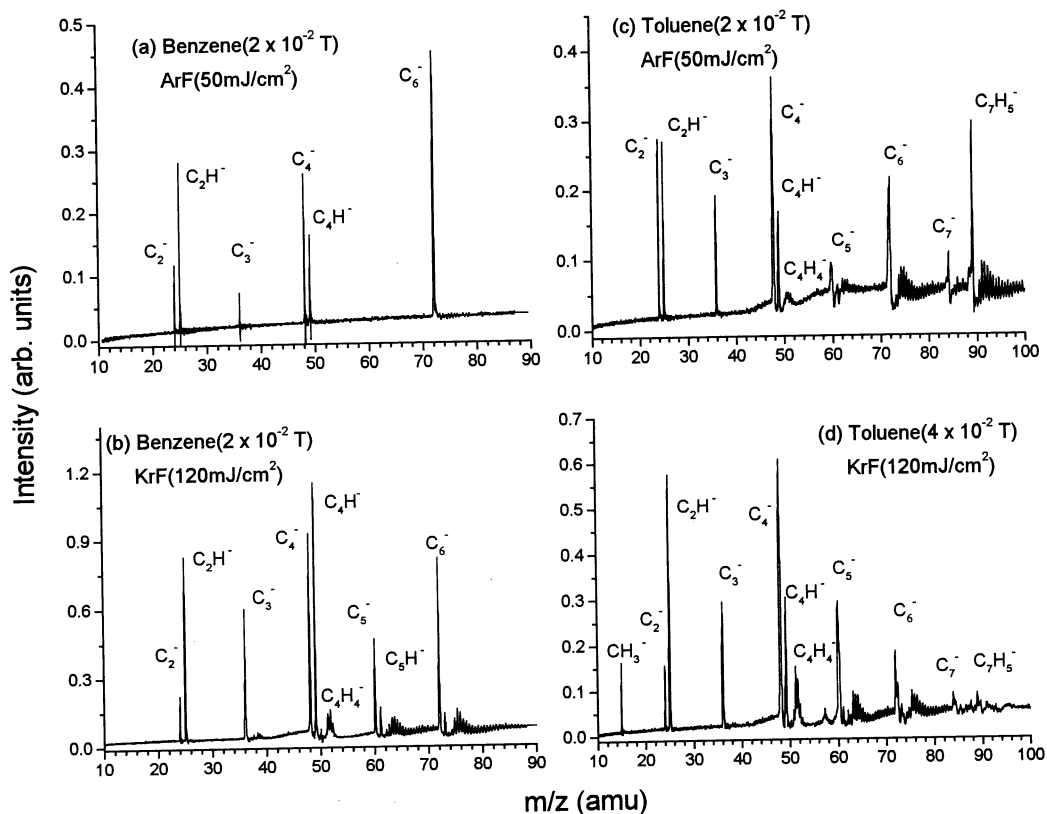
Fig. 4. Negative ion mass spectra for benzene and toluene at the ArF and KrF laser lines obtained with the pulsed beam valve arrangement. Note that estimated gas pressures in the laser interaction region (not the backing pressures in the beam valve) are shown.

to optimize the negative ion formation, the electric field in the laser region should be small during negative ion formation [6]; the superexcited HR state itself or the transient parent negative ion formed initially by the capture of the electron by the excited state is believed to be field ionized/detached at high electric fields [6,10].

The dynamics involving the superexcited HR molecules responsible for this enhanced electron attachment process, as well as the electron attachment characteristics, became clear [16] after the gas cell was replaced with the beam valve. In those experiments [16], we confirmed the long lifetimes of the superexcited HR states, which are required for subsequent negative ion formation by electron transfer to a second superexcited HR state [7]. The negative ion spectra obtained with the beam valve are shown in

Fig. 4. In this case, the negative ions produced by the laser pulse are pushed into the TOF by the use of only a single pulse that is applied to grid #1 a few microseconds after the laser pulse [see Fig. 2(b)]. Negative ions produced by the laser will remain in the region between the grids #1 and #2 until they are swept out of that region by the gas jet velocity.

Positive ion mass spectra, obtained under conditions similar to those for the data of Fig. 4, are shown in Fig. 5. A significant fraction of these positive ions have masses close to those of the molecular species. Laser multiphoton ionization of benzene has been studied by several groups. Reilly and Kompa [23] have measured positive ion spectra for benzene at the ArF and KrF laser lines, and those spectra are similar to the ones of Fig. 5.

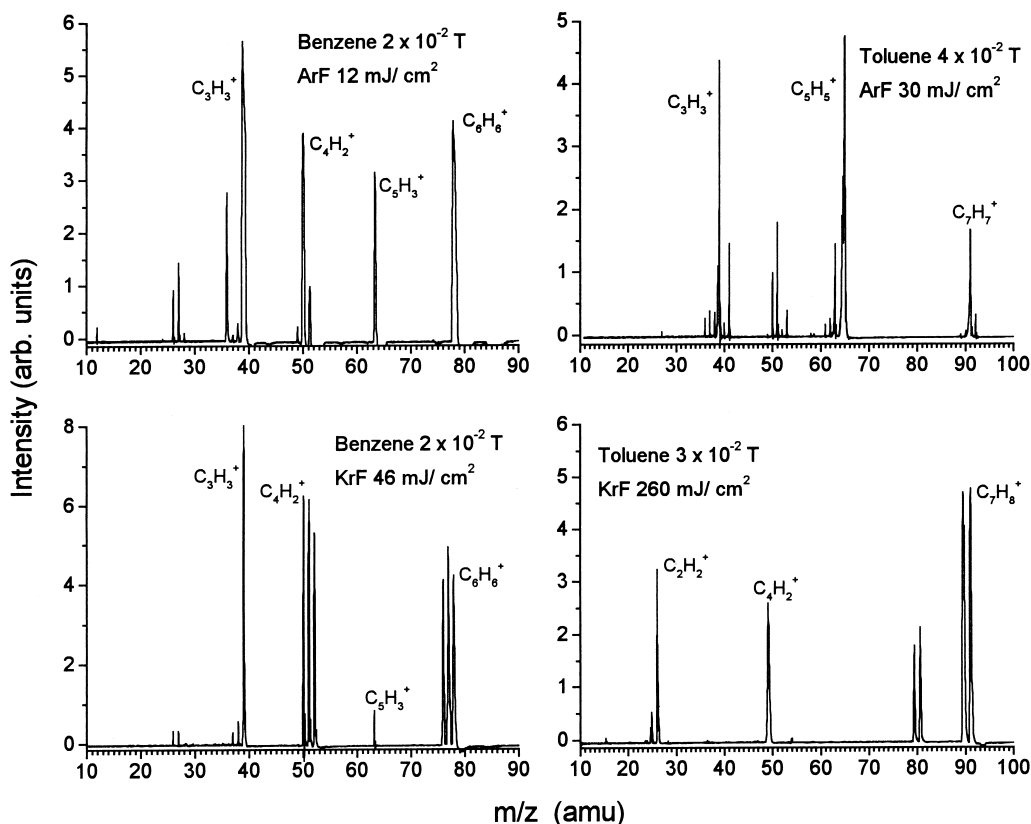A discussion is warranted on the wavelength de-

Fig. 5. Positive ion mass spectra for benzene and toluene at the ArF and KrF laser lines obtained with the pulsed beam valve arrangement. Note that estimated gas pressures in the laser interaction region (not the backing pressures in the beam valve) are shown.

pendence of the negative ion spectra in Fig. 4. More fragmentation was observed at the KrF line compared to the ArF line. Furthermore, this general fragmentation pattern did not change significantly over the intensity range where we observed negative ion formation. In the positive ion mass spectra, there is generally more fragmentation at the higher excitation energy (lower wavelength), and at a given excitation wavelength more fragmentation is observed at higher laser intensity. The positive ion mass spectra of Fig. 5 are consistent with the expected wavelength dependence, and we also observed higher fragmentation at higher laser intensities. The scenario in the negative ion formation, however, is different since it proceeds through intermediate dissociative parent negative ion states. The fragment anion pattern would depend on the asymptotic limits of the potential energy surfaces

along the dissociation pathways of these intermediate states. Therefore, although the fragmentation pattern can be expected to be dependent on the excitation energy, a certain trend with increasing excitation energy cannot be expected.

In our previous "high pressure" experiments [5,6] on electron attachment to laser-excited molecules, the electrons produced via photoionization drifted through the laser-excited molecules for ≈ 100 ns and attached to the excited molecules, which were shown to have lifetimes of the order of 100 ns. In the present experiments conducted under low pressure conditions (both gas cell and beam valve configurations) negative ion formation can also occur via the attachment of an electron from another close-by superexcited HR molecule [7] (as we mentioned above, the superexcited HR states were shown to have microsecond

lifetimes [16] under these low pressure conditions). This is quite similar to the pick up of a Rydberg electron from HR states of atoms by ground state molecules, see for example [24]. In the present case, a Rydberg electron is attached by another Rydberg molecular state.

It can be seen that the negative ions obtained with the beam valve are similar to those obtained with the gas cell; see Figs. 3 and 4. The characteristic pattern of mass peaks separated by mass of a carbon atom is quite clear. It must be noted that the effective gas pressure in the laser interaction region is about the same in both experimental arrangements. For the beam valve, the peak number density, ρ, of the gas at a distance, X, from the nozzle of diameter D is given by [25]

$$\rho = 0.16\rho_0[D/X]^2 \cos^2 \theta \qquad (2)$$

where, ρ_0 is the total pressure behind the nozzle and θ is the angle between the point of interest and the beam center line. For the backing pressure range of 2–40 Torr, $X = 1$ cm, and $D = 0.1$ cm, the local pressure at the laser interaction region is thus estimated to be in the range from $\approx 2 \times 10^{-3}$ to $\approx 4 \times 10^{-2}$ Torr. This is similar to pressure in the gas cell in the other experimental arrangement, see Fig. 2.

Negative and positive ion spectra as a function of the time delay between the extraction pulse and the laser pulse, obtained under comparable experimental conditions, are shown in Figs. 6 and 7. It can be seen that the negative ion spectra of Fig. 6 exhibit a larger number of distinct peaks than the positive ion spectra of Fig. 7. Although the intensity of the negative ion spectra is smaller, the intensity relative to the positive ion intensity is surprisingly large: The positive ions are produced via photoionization, which is the dominant process when a molecule is excited to an energy above its ionization threshold. As mentioned earlier, we estimate that only 10%–20% of the excitations for benzene at the KrF laser line end up in neutral superexcited states. Since the attaching electrons also need to come from these excited states, the probability for negative ion formation normally can be expected to be small. Yet, due to the extremely large cross
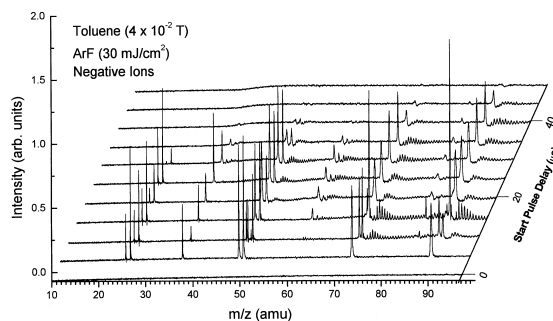

Fig. 6. Negative ion time-of-flight spectra for toluene at the ArF laser line with the pulsed beam valve arrangement illustrating the dependence of the ion intensities on the delay time between the laser pulse and the application of the start pulse to inject the ions to the TOF. At this laser line, the negative ions are formed ≈ 300 ns after firing of the laser pulse, and are present in the region between the grids #1 and #2 until they are removed by the gas jet velocity. Note that estimated gas pressures in the laser interaction region (not the backing pressures in the beam valve) are shown.

sections of the order of 10^{-10} cm^2 associated with this electron attachment process [6,26], the strength of the negative ion signal is within an order of magnitude of the strength of the positive ion signal. (The spectra of Figs. 6 and 7 were taken at a backing pressure of 40 Torr. It is likely that in the case of positive ion spectra
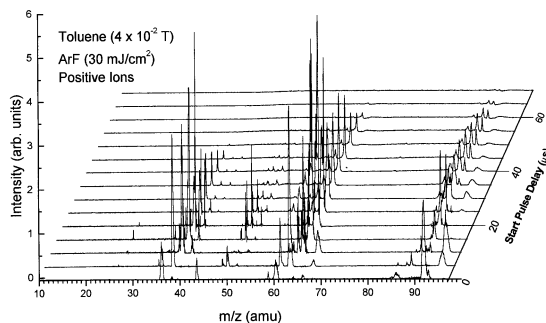

Fig. 7. Positive ion time-of-flight spectra for toluene under the same experimental conditions as those of Fig. 5. Most of the ion signals are saturated and thus the signal strengths for Figs. 5 and 6 cannot be compared. The signal strength for the positive ions at a pressure of 4×10^{-3} Torr were comparable to those of Fig. 5, and thus the negative ion strengths can be roughly stated to be about an order of magnitude smaller than the positive ions under similar conditions. Negative ion strengths can be improved by using external electrons for attachment, see the text. Note that estimated gas pressures in the laser interaction region (not the backing pressures in the beam valve) are shown.

of Fig. 7 the measured intensities are attenuated due to the saturation of the detector. The positive ion spectra for 4×10^{-3} Torr of toluene, with other parameters unchanged, yielded ion intensities comparable to the intensities of the negative ion spectra of Fig. 6. Thus, the negative ion spectra are roughly an order of magnitude less intense compared to the positive ion spectra at this laser intensity and pressure range.) It must be noted that although the positive ion signal is increased as PI^2, the negative ion signal increases as P^2I^4 [10]. The high efficiency of negative ion formation via this process was recently illustrated when it was shown that laser action in A1 can be obtained by charge neutralization of $A1^+$ ions by H^- ions produced via enhanced electron attachment to high-Rydberg states of H_2 [27].

The negative ion yield in electron attachment to laser-excited superexcited HR states has been shown [10] to vary as P^2I^4, where P is the gas pressure and I is the laser intensity. Such dependencies are difficult to be measured in the present experiments due to space charge effects. However, it was clear that the negative ion intensities varied nonlinearly with the pressure in contrast to positive ion intensities which varied almost linearly with the pressure (at very low gas pressures): To form one negative ion, at least two excited molecules are needed, one to provide the attaching excited molecule and the other to provide the electron for attachment. This requires fairly high densities of excited states (i.e. high laser fluences) in order to observe negative ion formation. It should be possible to form negative ions at lower laser fluences if external electrons can be provided for attachment. Such experiments are being planned.

To be of utility as an analytical tool, production of ions related to the molecular mass and/or structurally informative fragment ions must be produced. In the capture of an electron by a highly excited molecule, a transient parent negative ion is first produced [6]; due to the high internal energy of this parent negative ion, it dissociates rapidly leading to the formation of a stable fragment anion. It may be possible to stabilize the transient parent ion at higher ambient pressures, and thus to observe the parent negative ion. We plan to pursue this by increasing the pumping speed in the

gas cell arrangement and by providing an additional gas pulse in the pulsed valve arrangement. As for the fragment ions, we plan to study a variety of species to look for characteristic fragmentation patterns.

As mentioned earlier, enhanced electron attachment to molecules excited to energies above (and within a few electron volts of) the ionization threshold of a molecule appears to be a general phenomenon. We have observed efficient negative ion formation in H_2, NO, saturated tertiary amines, methane, silane; see [6] and references cited therein. Electron attachment to all these molecules in their ground states is weak, with rate constants of $<10^{-12}$ cm^3 s^{-1}. Fairly long-lived neutral superexcited states (which are core-excited high-Rydberg states) are responsible for the enhanced electron attachment observed in the laser experiments. The dissociative electron attachment to a molecule is energetically possible when

$$E_i + E_e > D(AB) - EA(B) \qquad (3)$$

where, E_i, E_e, $D(AB)$, and $EA(B)$ are the internal energy of the molecule, electron energy, dissociation energy of the molecule AB, and the electron affinity of B. Dissociation energies are normally ≤ 5 eV and the ionization thresholds (and hence the internal energy of a superexcited HR molecule) are almost always ≥ 7 eV. Hence electron attachment to superexcited states of molecules is energetically possible for any electron energy, including thermal-energy electrons where the electron capture is most efficient.

Most polyatomic molecules have ionization thresholds between ≈ 6 and ≈ 12 eV. Furthermore, in most molecules the first electronically excited state lies around or below one-half of the ionization energy, and thus two-photon excitation of molecules to energies above their ionization thresholds is possible using UV lasers (photon energy in the range from ≈ 3.5 to ≈ 6.4 eV). Especially for larger polyatomic molecules, the density of the excited states at the one-photon energy level is high which can lead to efficient resonant two-photon absorption. Therefore, commonly available lasers such as excimer lasers or frequency-quadrupled Nd:YAG lasers can be used to excite molecules to energies above their ionization

thresholds. Since the population of superexcited HR states seems to be guaranteed at any energy (within a few electron volts) above the ionization threshold, tunable lasers are not necessary. However, as in positive ion mass spectrometry, tunable lasers can be used to achieve spectral selection of a compound prior to mass analysis. Furthermore, the ability to generate both positive and negative ion spectra will be another advantage of this technique. Further studies are needed to evaluate the potential of this technique as an analytical technique.

4. Conclusions

We have presented negative ion spectra of benzene and toluene that resulted from enhanced electron attachment to high-Rydberg states of those molecules. These experiments illustrate that fragment negative ions of benzene and toluene can be produced efficiently via this laser-enhanced electron attachment process than by electron attachment to their ground electronic states. Further studies are needed to evaluate the potential of this technique as an analytical technique.

Acknowledgements

References

[1] H. Budzikiewicz, Angew. Chem. Int. Ed. Engl. 20 (1981) 624.
[2] A.G. Harrison, Chemical Ionization Mass Spectrometry, CRC, Boca Raton, FL, 1983.
[3] M.V. Buchanan, G. Olerich, Org. Mass Spectrom. 19 (1984) 486.
[4] L.G. Christophorou, D.L. McCorkle, A.A. Christodoulides, in Electron-Molecule Interactions and Their Applications, L.G. Christophorou (Ed.), Academic, New York, 1984.
[5] L.A. Pinnaduwage, P.G. Datskos, J. Chem. Phys. 104 (1996) 8382.
[6] L.A. Pinnaduwage, P.G. Datskos, J. Appl. Phys. 81 (1997) 7715.
[7] K. Nagesha, L.A. Pinnaduwage, J. Chem. Phys. 109 (1998) 7124.
[8] L.A. Pinnaduwage, W. Ding, D.L. McCorkle, Appl. Phys. Lett. 71 (1997) 3634.
[9] W.X. Ding, D.M. McCorkle, L.A. Pinnaduwage, J. Appl. Phys. 84 (1998) 3051.
[10] L.A. Pinnaduwage, L.G. Christophorou, A.P. Bitouni, J. Chem. Phys. 95 (1991) 274.
[11] J.A.D. Stockdale, R.N. Compton, P.W. Reinhardt, Int. J. Mass Spectrom. Ion Processes 4 (1970) 401.
[12] H.P. Fenzlaff, E. Illenberger, Int. J. Mass Spectrom. Ion Phys. 59 (1984) 185.
[13] R.C. Dougherty, C.R. Weisenberger, J. Am. Chem. Soc. 90 (1968) 6570.
[14] R.T. Aplin, H. Budzikiewicz, C. Djerassi, J. Am. Chem. Soc. 87 (1965) 3180.
[15] R.L. Platzman, Radiation Res. 17 (1962) 419.
[16] L.A. Pinnaduwage, Y. Zhu, Chem. Phys. Lett. 277 (1997) 147.
[17] W.G. Scherzer, H.L. Selzle, E.W. Schlag, Z. Naturforsch. 48A (1993) 1256.
[18] W.G. Scherzer, H.L. Selzle, E.W. Schlag, R.D. Levine, Phys. Rev. Lett. 72 (1994) 1435.
[19] H. Matsui, J.M. Behm, E.R. Grant, J. Phys. Chem. A 101 (1997) 6717.
[20] F. Ramacle, R.D. Levine, E.W. Schlag, H.L. Selzle, A. Held, J. Phys. Chem. 100 (1996) 15320.
[21] L.A. Pinnaduwage, D.L. McCorkle, Chem. Phys. Lett. 255 (1996) 410.
[22] L.A. Pinnaduwage, Y. Zhu, J. Chem. Phys. 108 (1998) 6633.
[23] J.P. Reilly, K.L. Kompa, J. Chem. Phys. 73 (1980) 5468.
[24] C.D. Finch, R. Parthasarathy, H.C. Akpati, P. Norlander, F.B. Dunning, J. Chem. Phys. 106 (1997) 9594.
[25] D.H. Levy, L. Wharton, R.E. Smalley, Chemical and Biochemical Applications of Lasers, C.B. Moore (Ed.), Academic, New York, 1977, Vol. 1, p. 1.
[26] L.A. Pinnaduwage, W. Ding, D.M. McCorkle, S.H. Lin, A.M. Mebel, A. Garscadden, J. Appl. Phys. 85 (1999) 7064.
[27] J.F. Kielkopf, L.A. Pinnaduwage, L.G. Christophorou, Phys. Rev. A 49 (1994) 2675.